Terahertz-metallic aperture arrays designing

Binbin Li (李宾宾)[1], Shengmei Yan (严胜美)[2], Wei Xiong (熊 伟)[2], Jingling Shen (沈京玲)[1*], and Jun Yao (姚 军)[2]

[1]*Beijing Key Laboratory for Terahertz Spectroscopy and Imaging, Key Laboratory of Terahertz Optoelectronics, Ministry of Education, Department of Physics, Capital Normal University, Beijing 100048, China*

[2]*State Key Lab of Optical Technologies for Microfabrication, Institute of Optics and Electronics, Chinese Academy of Sciences, Chengdu 610209, China*

[*]*Corresponding author: jinglingshen@gmail.com*

Received December 30, 2011; accepted February 23, 2012; posted online June 20, 2012

A Terahertz sensing method based on the resonant transmission characteristics through metallic aperture arrays is proposed. Here we present metallic aperture arrays of rectangular and H-shaped holes which induce localized resonance. High characterization sensitivity to surface condition is demonstrated. When applied with the liquid of 3-pentanone, arrays of rectangular and H-shaped holes have sensitivity of 158 and 172 GHz/RIU (refractive index unit), respectively. So the metal meshes based localized resonance can also be used as a sensor chip in terahertz region.

OCIS codes: 310.6845, 310.6628, 240.0240.
doi: 10.3788/COL201210.S13102.

Terahertz technology has a broad applicability in the biomedical context because the collective vibration modes of many protein and DNA molecules are predicted to occur in terahertz range. In recent years the rapid development of terahertz technology in expanding sensing methods and improving sensor precision brings hope and motivation. Because of its unique properties, it has broad application prospects in physics, chemistry, biological medicine, communications, radar, safety inspection, and so on[1,2]. One of those unique properties is that interactions between terahertz wave and metallic aperture array produce abnormal transmission phenomenon[3−6]. The resonance conditions of producing surface plasmon resonance (SPR) can be achieved by carving out with periodic holes of subwavelength size in metal surface[7,8]. The metallic aperture array is very sensitive to environmental media and has potential utility in immunoassays and other biochemical sensing applications[9]. This label-free detection method with terahertz wave is a convenient technique with high sensitivity in biomedicine, which enables us to realize easier and faster medical and food inspections than other techniques. In addition, metal structure size is in sub-millimeter range, so we do not need to make metallic nano structure, simple to implement.

The application of SPR in terahertz band has been made lots of efforts[7,8]. The theoretical and experimental results show that terahertz transmission has a strong increase in the resonant frequency through a metallic aperture array, this is due to the metallic aperture array adjusted dielectric constant of metal. It actually realized function of artificial electromagnetic material. A label-free sensing method using a metallic aperture array of subwavelength hole in terahertz region has been proposed these years[9−11]. The resonant transmission properties of electromagnetic waves are attributed to surface waves, which is due to the phenomenon of SPR. In this letter, we report terahertz sensing chips of metallic aperture arrays of rectangular holes (mesh A) and H-shaped holes (mesh B). The resonant frequency of terahertz transmission spectrum is due to localized resonance. In this case, surface plasmon is limited in the hole instead of spreading in the metal surface. The experimental results show that the transmission properties caused by localized resonance also sensitive to environmental media, that is, when a sample substance is applied on the mesh openings, resonant frequency red-shift as the increase of the refractive index near the surface boundary.

The structure of a sensing chip consists of metallic aperture array patterned on a high-resistivity silicon substrate. The metal layer is chosen to be 500-nm-thick chromium, and the thickness of the silicon substrate is 380 μm. The two arrays with different apertures of rectangular and H-shaped distribute along a square grid. The lattice constant T of the two arrays is 140 μm, the length of rectangular holes L is 120 μm, the width G is 20 μm, and the width of H-shaped aperture K is 10 μm. The parameters of a unit cell are shown in Fig. 1.

Terahertz transmission characteristics are analyzed by the finite-difference time-domain (FDTD) simulation. In the simulation, we described the metallic aperture array by surrounding a unit cell with periodic boundary conditions on the four sidewalls. The material of the metal layer is assumed to be perfect electric conductor. Due to drastic increase in the value of complex permittivity, most metals become highly conductive at terahertz frequencies. The substrate was modeled as lossless silicon with refractive index of 3.42. The simulation of the 500-nm-thick layer required extremely large computer memory and time, so the metal layer thickness was set to be 2 μm to simplify the problem. This thickness change is based on the fact that the resonance peaks vary little as thickness increase to larger values in our multiple simulations. The simulated transmission spectra through the metallic aperture arrays are shown as solid line in Fig. 2. The resonance peaks observed

 © 2012 Chinese Optics Letters

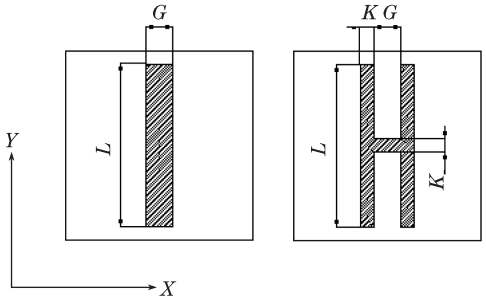

Fig. 1. Parameters of rectangular and H-shaped hole: $L = 120\ \mu$m, $G = 20\ \mu$m, and $K = 10\ \mu$m.

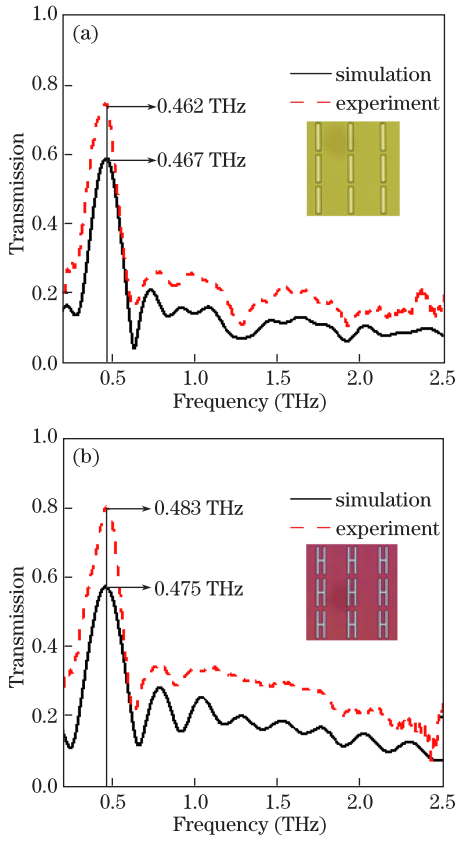

Fig. 2. Transmission spectra through metal meshes (a) A and (b) B. Inset: part of the scanning electron microscope (SEM) image of the metal arrays.

at 0.467 and 0.475 THz for meshes A and B, respectively.

The sensing chips are fabricated by conventional photolithography techniques. They are characterized in transmission by terahertz time-domain spectroscopy (THz-TDS). The schematic experimental THz-TDS setup is shown in Fig. 3. Fiber femtosecond laser (Fx-100, IMRA) with 113-fs pulse duration, 800-nm central wavelength, 75-MHz repetition rate, and 120-mW output power was used as the laser source for pumping and detecting terahertz pulses. In the system a photoconductive antenna (PCA) is used as the emitter, a ZnTe crystal as the detector. The dynamic range is greater than 1 000 and the signal-to-noise ratio (SNR) at the peak value position is about 400[12]. THz-TDS allowed us to directly measure the waveform of the terahertz wave in time domain. We got the transmission spectra by Fourier transform of time domain waveforms. The metallic mesh

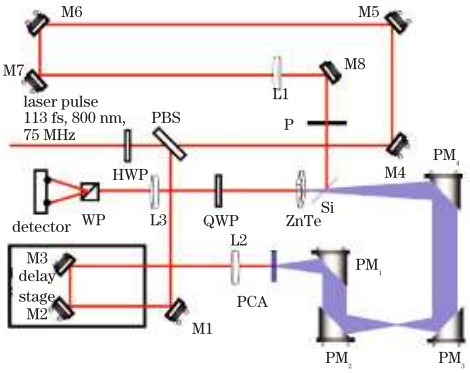

Fig. 3. Schematic experimental THz-TDS setup.

is penetrated by the focused terahertz beam at normal incidence and with the polarization along X axis. The transmission is defined as $\left|\widetilde{t}(\omega)\right| = \left|E_{\rm sam}(\omega)/E_{\rm ref}(\omega)\right|$, where $E_{\rm sam}(\omega)$ and $E_{\rm ref}(\omega)$ are the Fourier-transformed frequency-dependent amplitudes of the terahertz pulses with and without the metal meshes, respectively. The transmission spectra of the metal meshes are shown as dashed line in Fig. 2. The measured resonant frequencies are 0.462 and 0.483 THz for meshes A and B, respectively. They are in good agreement with the simulation results. The difference between resonant frequencies is due to the different thicknesses of metal layer between simulation and real values. The oscillation between 0.6 and 2.5 THz is caused by scattering of surface mesh and the fabry-perot oscillation of substrates.

When a light wave is incident upon the surface of a metallic circle hole array, surface-plasmon polaritons (SPPs) can be resonantly excited along the metal-dielectric interface if the following momentum match is conserved[6,13]:

$$K_{\rm sp} = K_{\rm II} + G, \tag{1}$$

where $K_{\rm sp}$ is the wave vector of SPPs; $K_{\rm II}$ is the in-plane wave vector with $K_{\rm II}(\omega/\ c)\sin\ \theta$, in which θ is the incidence angle, and c is the speed of light in free space; G is the reciprocal lattice vector of the periodic structure, $G = 2\pi(m^2 + n^2)^{1/2}/T$ for a square lattice, where m and n are integers corresponding to the specific order of the SPP. Additionally, the wave vector of SPPs, $K_{\rm sp}$, yields the general dispersion relation[6,13]:

$$K_{\rm sp} = \frac{\omega}{c}\left(\frac{\varepsilon_{\rm d}\,\varepsilon_{\rm m}}{\varepsilon_{\rm d} + \varepsilon_{\rm m}}\right)^{1/2}, \tag{2}$$

where $\varepsilon_{\rm m}$ and $\varepsilon_{\rm d}$ are the dielectric constants of the constituent metal and dielectric, respectively, and $-\varepsilon_{\rm m} >> \varepsilon_{\rm d}$. If the thickness of the dielectric is assumed to be infinite, the (1, 0) SPP mode could exhibit a resonance frequencies at a particular value of $\varepsilon_{\rm d}({n_{\rm d}}^2)$. By solving Eqs. (1) and (2), resonance frequencies of surface waves can be predicted

$$f_{\rm sp}^{m,n} = (c/T)\,\varepsilon_{\rm d}^{-1/2}. \tag{3}$$

So the resonance frequency mainly depends on refractive index of the adjacent medium and the lattice constant T. When a material is placed near the mesh, the transmission properties of a metallic mesh are affected by the refractive index of that material, in the sense that a shift of the transmission peak occurs. With this surface

plasmon enhanced terahertz spectroscopic identification, metallic aperture arrays of subwavelength circular holes have been proved to be a good biochemical sensor[9,10].

The real peak position appears in Fig. 2 is different from calculated resonance frequencies of surface waves through Eq. (3). This is because the localized resonance mode dominates the transmission through our structure. Very recently, many studies have investigated the effects of hole size on transmission characteristics, and experimentally found that the hole shape also has a strong effect on the transmission characteristics of metal hole arrays[14−16]. This effect is known as localized resonance, and it has been investigated extensively[17]. Large enhancement in transmission intensity has been shown to appear when the polarization of the incident light is perpendicular to long edge of rectangular holes. Miyamaru *et al.* has indicated that as the length (long edge) of rectangular holes decreases, the dominant resonant transmission mechanism changes from localized resonance to surface waves. When the length of rectangular metal hole is more than the half-period, the resonant peak clearly depends on the length of rectangular metal holes. The peak frequency is equal to the expected frequency of the half-wavelength resonance in the free-standing structure: $f_{\rm loc} = c/2L$[17]. As his result, different from excitation of surface waves on the surface of the circle hole array, the dominant resonant transmission mechanism for our structure is localized resonance, due to the length of samples L (120 μm) is greater than the half-period ($T/2$=70 μm).

Different from SPR, which is a kind of conduction mode, localized SPR (LSPR) is limited in all kinds of different shape of local hole. This can cause enhancement effect of significant energy in local area. We have designed four kinds of metal structure as shown in illustrations of Fig. 4. They have the same length L (120 μm) perpendicular to the polarization of the incident terahertz. The characteristics of transmission are basically same as shown in Fig. 4. Because LSPR has not much relationship with shape of hole, it depends on length of local area.

Though the transmission mechanism is different, the extraordinary transmission characteristics based on localized resonance mode also have sensitivity to the surrounding media as same to metallic circle hole arrays. We have detected liquid of 3-pentanone, which is used to change the permittivity above the metal surface. 3-pentanone is a kind of organic solvents and intermediate of drug synthesis. Its optical parameters have been measured in our system already, refractive index of 3-pentanone is 1.167 at 1.0 THz. In the detecting experiment, the reference is terahertz pulses transmitted through an empty quartz cell, which is used as a container of the liquid, at normal incidence. In this direction, the quartz cell is composed of two parallel quartz walls with 1-mm thick and a 0.9-mm space. Firstly, the sensing chip was put inside the empty quartz cell, and kept the metal mesh surface contact with air and the substrate contact with the cell wall. The transmission spectra measured are shown as solid line in Fig. 5. Then the liquid of 3-pentanone was injected in the quartz cell instead of the air around the metal mesh. In this case, the measured transmission spectra of terahertz wave through the sensing chips are illustrated as dotted line in Fig. 5.

As shown in Fig. 5(a), resonance peak of transmission spectra shifts from 0.455 to 0.428 THz as the air on the surface of sensing chip be substituted by 3-pentanone; for sensing chip B, resonance frequency shifts from 0.476 to 0.447 THz, as shown in Fig. 5(b). In addition, the resonance amplitude reduced in 3-pentanone due to the liquid absorption. We use $S = \Delta f/\Delta n$ to evaluate refractive index sensitivity of the structure, which represents the resolution of resonance frequency per refractive index unit (RIU)[18,19]. Sensitivities for sensors A and B are 158 and 172 GHz/RIU, respectively (refractive index of air is 1 and refractive index of 3-pentanone is 1.167 at 1.0 THz). Clearly, transmission characteristics of subwavelength structure based on localized resonance are also significantly modified by the existing ambient media, the resonant frequencies of the transmission peak strongly depend on the refractive index in the vicinity of the metallic mesh openings. The thickness of 3-pentanone on the metal film is less than 500 μm, so a

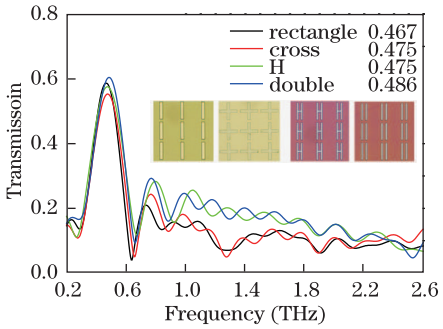

Fig. 4. Transmission spectra of four metal structures.

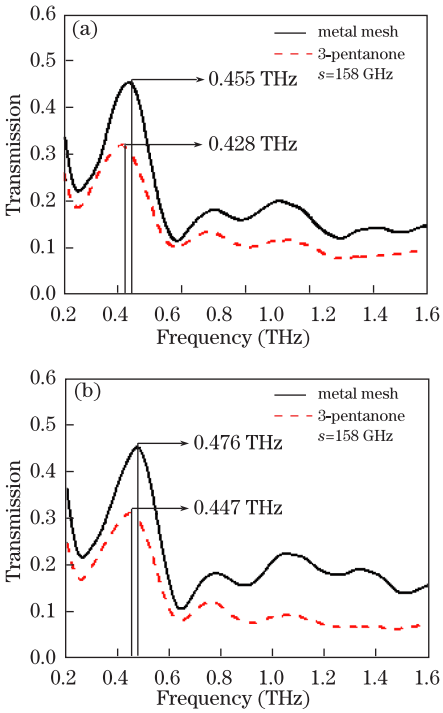

Fig. 5. Measured transmission spectra through metal meshes (a) A and (b) B.

considerably small amount of sample spread on the metal film can be detected.

As a mechanism of localized resonance, the peak frequencies of the measured transmission spectra are indicated by open circles. Transmission peaks appear at the $f_{\rm loc} = c/2L$ in the free-standing structure[17]. But in our sample this value should be divided by the effective refractive index $n_{\rm eff} = \left(\frac{n_1^2+n_2^2}{2}\right)^{1/2}$ since the metallic periodic structure is sandwiched between the Si substrate and air[20]:

$$f_{\rm loc} \approx c/2Ln_{\rm eff}, \quad (4)$$

and the refraction index of air (n_1) is 1, the refraction index of substrates Si (n_2) is 3.42. From Eq. (4), the theoretical resonance peak is estimated to be 0.496 THz. The measured values for meshes A and B are 0.462 and 0.483 THz, respectively, are slightly smaller than the theoretical value.

When the metal film is submerged in liquid of 3-pentanone, the spectra show that transmission peaks redshift when the air ($n_1 = 1$) is replaced by 3-pentanone ($n_1' = 1.167$), because the transmission characteristics affected by an increased refraction index of material on the meshes, resonance frequency is modulated according to Eq. (4). We have experimentally demonstrated a high sensitivity in detecting liquid of 3-pentanone, the refraction index of which is close to air. This indicates that localized resonance phenomenon can also be used in detection.

For an idealized structure, the resonance peak could shift obvious when the refractive index changes, what we are looking for. Our mesh B shows higher sensitivity than mesh A, the difference of sensitivity between the two structures with the same length L probably due to different field enhancements through the structures. LSPR in H-shaped array can cause more significant energy of enhancement effect in local area compared to rectangular array, so the shape of structure affects the sensitivity of a sensing chip.

In conclusion, we design subwavelength holes of rectangular and H-shaped in terahertz band. The simulated terahertz transmission spectra of meshes are consistent with experimental measured values through our THz-TDS. Different from a metallic aperture array of circle apertures which induce SPR, the dominant mechanism for our metallic aperture arrays is localized resonance, due to the length of rectangular holes L is more than the half-period and the peak frequency is equal to the expected frequency of the half-wavelength resonance. We also demonstrate that the transmission properties are also affected by the refractive index of that material placed near the mesh openings, even a small amount. In detecting the liquid of 3-pentanone less than 500 μm, the metallic aperture arrays show high sensitivity. H-shaped holes array has a higher sensitivity (172 GHz/RIU) relative to array of rectangular holes (158 GHz/RIU).

This work was supported by the Natural Science Foundation of Beijing (No. 4102016) and the Science and Technology Program of Beijing Educational Committee (No. KM200910028005).

References

1. N. Karpowicz, H. Zhong, C. L. Zhang, K.-I Lin, J.-S. Hwang, J. Xu, and X.-C. Zhang, Appl. Phys. Lett. **86,** 054105 (2005).
2. H. Zhong, A. Sanchez, and X.-C. Zhang, Opt. Express **14,** 9130 (2006).
3. D. E. Grupp, H. J. Lezec, T. W. Ebbesen, K. M. Pellerin, and T. Thio, Appl. Phys. Lett. **77,** 1569 (2000).
4. A. Krishnan, T. Thio, T. J. Kim, H. J. Lezec, T. W. Ebbesen, P. A. Wolff, J. B. Pendry, L. Martín-Moreno, and F. J. García-Vidal, Opt. Commun. **200,** 1 (2001).
5. L. Martín-Moreno, F. J. García-Vidal, H. J. Lezec, K. M. Pellerin, T. Thio, J. B. Pendry, and T. W. Ebbesen, Phys. Rev. Lett. **86,** 1114 (2001).
6. H. Raether, *Surface Plasmons on Smooth and Rough Surfaces and on Gratings* (Springer-Verlag, Berlin, 1988).
7. D. Qu, D. Grischkowsky, and W. Zhang, Opt. Lett. **29,** 896 (2004).
8. A. K. Azad, M. He, Y. Zhao, and W. Zhang, Opt. Lett. **31**, 2637 (2006).
9. F. Miyamaru, S. Hayashi, C. Otani, K. Kawase, Y. Ogawa, H. Yoshida, and E. Kato, Opt. Lett. **31,** 1118 (2006).
10. Z. Tian, J. Han, X. Lu, J. Gu, Q. Xing, and W. Zhang, Chem. Phys. Lett. **475,** 132 (2009).
11. H. Yoshida, Y. Ogawa, Y. Kawai, S. Hayashi, A. Hayashi, C. Otani, E. Kato, F. Miyamaru, and K. Kawase, Appl. Phys. Lett. **91,** 253901 (2007).
12. M. Naftaly and R. Dudley, Opt. Lett. **34,** 1213 (2009).
13. H. F. Ghaemi, T. Thio, D. E. Grupp, T. W. Ebbesen, and H. J. Lezec, Phys. Rev. B **58,** 6779 (1998).
14. K. L. Van der Molen, K. J. K. Koerkamp, S. Enoch, F. B. Segerink1, N. F. van Hulst, and L. Kuipers, Phys. Rev. B **72,** 045421 (2005).
15. Z. Ruan and M. Qiu, Phys. Rev. Lett. **96,** 233901 (2006).
16. J. Han, A. K. Azad, M. Gong, X. Lu, and W. Zhang, Appl. Phys. Lett. **91,** 071122 (2007).
17. F. Miyamaru and M. W. Takeda, Phys. Rev. B **79,** 153405 (2009).
18. J. Han, A. K. Azad, M. Gong, X. Lu, and W. Zhang, Appl. Phys. Lett. **91,** 071122 (2007).
19. A. D. McFarland and R. P. Van Duyne, Nano Lett. **3,** 1057 (2003).
20. Y. W. Jiang, L. D. Tzuang, Y. H. Ye, Y. T. Wu, M. W. Tsai, C. Y. Chen, and S. C. Lee , Opt. Express **17,** 2631 (2009).